JOURNAL OF GUIDANCE, CONTROL, AND DYNAMICS
Vol. 27, No. 5, September–October 2004

Libration Control of Flexible Tethers Using Electromagnetic Forces and Movable Attachment

Paul Williams*
RMIT University, McKinnon, Melbourne 3204, Australia
Takeo Watanabe†
Tokyo Metropolitan Institute of Technology, Tokyo 191-0065, Japan
Chris Blanksby‡ and Pavel Trivailo§
RMIT University, McKinnon, Melbourne 3204, Australia
and
Hironori A. Fujii¶
Tokyo Metropolitan Institute of Technology, Tokyo 191-0065, Japan

This paper proposes utilizing the distributed Lorentz forces that are induced in an electromagnetic tether as a control actuator for controlling the tether motion. The control input governing the magnitude of the applied actuator force is the current being conducted within the tether. A wave-absorbing controller is also proposed to suppress the unstable high-order modes that tend to be initiated by electromagnetic forces. The absorption of traveling waves along the tether can be achieved by proper movement of the tether attachment point on the main satellite. A mission function control law is presented for controlling the tether length and in- and out-of-plane librations, derived from a model that treats the tether as an inextensible rigid rod. The control law is numerically simulated in a continuum model of the tether system. It is shown that the out-of-plane motion of the tether can be effectively damped by appropriate control of the tether current for inclined orbits. The presence of tether flexibility causes significant bowing of the tether that grows into instability of the lateral modes. It is shown that this instability can be effectively suppressed by applying the proposed wave-absorbing controller for deployment, retrieval, and stationkeeping scenarios.

I. Introduction

THE idea of using of tethers in space missions has grown considerably in the last two decades. Originally, the Smithsonian Astrophysical Observatory[1] suggested using a space-shuttle-supported tethered satellite system to perform measurements of the upper atmosphere. An investigation into the dynamics of the so-called "Skyhook" project[2] and the corresponding published results brought forth a myriad of more advanced proposed applications. Some of these applications include momentum transfer,[3–5] electrodynamic reboost of the International Space Station,[6–7] payload capture[8] and deorbit,[9–10] and aerobraking.[11–12]

Electromagnetic tethers have been proposed as a means for providing propellantless propulsion for both orbital boost and deorbit of spent satellites. In particular, they are an efficient means for reboosting the orbit of the International Space Station[6,7] and for deorbiting satellites at the end of their operational life.[13] Although these applications require control because of the inherent instability of electromagnetic tethers, very little research has gone into developing electromagnetic forces as a control actuator. It is proposed that utilizing the distributed electromagnetic Lorentz forces on a conductive tether might be an alternative to employing thrusters on the subsatellite to control the out-of-plane librational motion of the tether. One of the concerns with using electromagnetic forces is the potential for the excitation of unstable high-order modes of vibration. These modes are very difficult to control by electromagnetic forces alone because the feedback of modal amplitudes, as suggested by Ruiz et al.,[14] would be impractical. Even if this were possible, however, the ability to damp out high-order modes with a distributed force that varies in direction with the local shape of the tether is yet to be established as practical. This paper proposes an alternative method for damping out the higher-order modes of vibration by adjusting the system boundary conditions. This additional control actuator requires only measurement of the tether dynamics at the attachment point.

The main purpose of the study proposed in this paper is for the evaluation of actuation methods for manipulating the tip position of tethered systems. Some proposed applications of tethered systems including the capture and deorbit, or capture and boosting of payloads via momentum transfer, will require control systems capable of manipulating the motion of the tether in all three spatial dimensions. The long-term viability of such systems will be dependent on the requirements for chemical propellant. Electrodynamic tethers can provide a means for satisfying several requirements for such systems, including control of the librational motion. The purpose of this paper is to assess the dynamics of a tethered system when electromagnetic forces are used as a control actuator.

An excellent survey of the work done on cable-connected space bodies has been undertaken by Misra and Modi.[15] A good summary of the work done on deployment and retrieval control laws is available in this reference, including various forms of Rupp's tension control laws.[16] The most significant control work on tethered systems has been to stabilize the retrieval phase, because this is naturally unstable. This work has included the nonlinear feedback of out-of-plane librations[17] as well as the modal amplitudes of transverse vibrations.[18]

Deployment and retrieval of a tethered subsatellite has been considered by a number of authors[19,20] using a number of proposed additional control actuators, including the use of a crawler on the

Received 14 April 2003; presented as Paper 2003-5781 at the AIAA Guidance, Navigation, and Control Conference and Exhibit, Austin, TX, 11 August 2003; revision received 15 September 2003; accepted for publication 14 January 2004.

*Ph.D. Candidate, Department of Aerospace Engineering. Student Member AIAA.
†Ph.D. Candidate, Department of Aerospace Engineering.
‡Senior Research Fellow, Department of Aerospace Engineering.
§Professor, Department of Aerospace Engineering.
¶Professor, Department of Aerospace Engineering. Associate Fellow AIAA.

tether[21] and the use of thrusters to augment the vibrations of the tether during retrieval.[22,23] Chu and Wang[24] have presented alternative deployment and retrieval strategies that keep the tether slack through the main deployment/retrieval process. A number of authors have employed the Lyapunov design (mission function[25,26]) approach to stabilize deployment and retrieval[26–30] to track an optimal path[31,32] and to control multitethered satellite systems.[30] The nonlinear attitude control of space-platform-based tethered systems has been considered by Modi et al.,[33] who also used Lyapunov control techniques.

Pradhan et al.[34,35] consider the control of a rigid body-elastic tether system using movement of an offset attachment point as the actuator. The controller is designed using a feedback linearization technique. The general method is validated using a ground-based experimental test rig, which emulates the basic features of the space tether system. In Ref. 35, Pradhan et al. use offset control to control the librations and transverse vibrations of a tethered system. The ability to control tether librations using offset control alone is limited by the maximum displacement of the attachment point, because the ratio of offset distance to tether length is very small for most practical tether systems. The controller is designed using a linear quadratic Gaussian loop transfer recovery (LTR) approach considering only the first mode of vibrations. In this paper, we propose a fundamentally different control approach for controlling the transverse vibrations using the attachment point as a control input, and we also consider the external load caused by electromagnetic forces.

Although the dynamics of electrodynamic tethers have been studied previously,[36–41] only a small number of papers have dealt with using electromagnetic forces as a control actuator. Netzer and Kane[42] consider controlling the dynamics of an electrodynamic tether using the combination of current and thruster control. The control objective is to keep the tether Earth pointing, and no changes in tether length are considered. A simple system model consisting of equal end masses and a single point mass connected by massless rods—representing the tether—is used in their study. The controller is designed using a linearized set of equations through the application of linear quadratic regulator theory. The results are promising but limited by the assumption of a nonflexible fixed length tether. The combined use of length rate and current control is considered by Tani and Qui,[43] who employ a massless two-dimensional tether model and a proportional-derivative controller.

The design and implementation of a nonlinear controller incorporating electromagnetic Lorentz forces in a fully flexible three-dimensional model of the tether system has not yet been undertaken. This paper deals with precisely this issue.

II. Mathematical Models

A. Tether as a Rigid Rod

In general, tether dynamics are very complex. A flexible tether undergoes a complicated set of coupled vibrations. These can be separated into longitudinal, lateral, and rigid-body modes. All three of these vibratory modes are coupled as a result of the influence of the gravity-gradient and system nonlinearities. Although a detailed study of tether dynamics must inevitably account for the entire range of vibrations, the initial feasibility of a concept and/or design of a controller can be established/rejected using only a simplified model. In this study, a model of the tether dynamics that neglects tether flexibility is adopted for the control law design. Such models are often used in tether control law design because of their simplified mathematical representations and computational efficiency.

The major assumptions employed in the derivation of the mathematical model are that 1) the tether is rigid, inextensible, but can vary in length in a controlled manner; 2) the only external forces acting on the tether system are the Newtonian gravity force and electromagnetic Lorentz forces, and aerodynamic drag and solar pressure forces are considered negligible; 3) the end masses are considered to be point masses; 4) the tether is uniform in mass; 5) the tether is deployed/retracted from one end mass only; 6) the mother satellite is significantly greater in mass than the tether or the subsatellite, and consequently the center of mass of the system can be assumed to coincide with the center of mass of the mother satellite; and 7) the mother satellite remains in an unperturbed circular orbit.

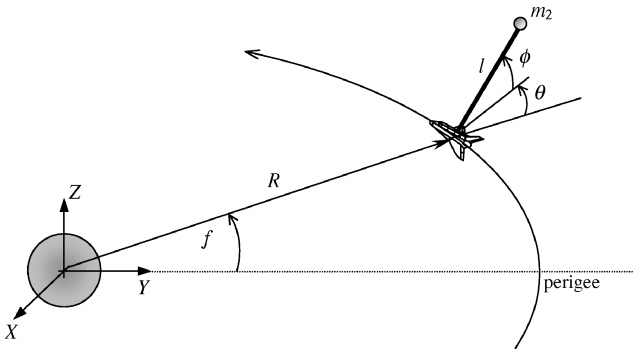

Fig. 1a Simplified representation of a tethered satellite system, modeled with point masses and an inextensible rigid rod.

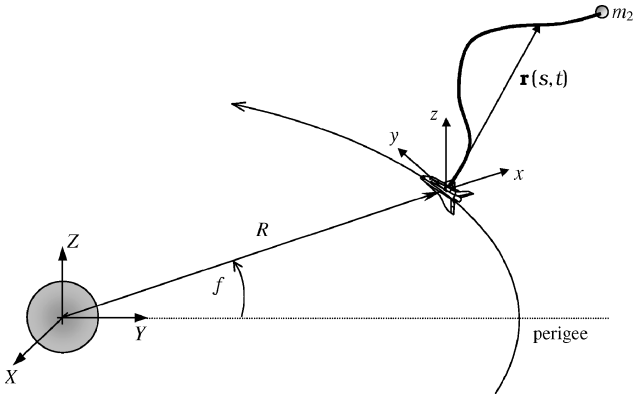

Fig. 1b Continuum model of a tethered satellite system.

A representation of the model, as well as the generalized coordinates used to describe the motion, is shown in Fig. 1a. The generalized coordinates are selected as the in-plane tether libration angle θ, the out-of-plane tether libration angle ϕ, and the tether length l. Application of Lagrange's equations leads to the following nondimensional equations of motion:

$$\theta'' = 2(\theta'+1)[\phi' \tan\phi - \Gamma_1(\lambda'/\lambda)] - 3\sin\theta\cos\theta + Q_\theta \Big/ (m_2 + m_t/3)\lambda^2 L_f^2 \omega^2 \cos^2\phi \tag{1}$$

$$\phi'' = -2\Gamma_1(\lambda'/\lambda)\phi' - [(\theta'+1)^2 + 3\cos^2\theta]\sin\phi\cos\phi + Q_\phi \Big/ (m_2 + m_t/3)\lambda^2 L_f^2 \omega^2 \tag{2}$$

$$\lambda'' = -\Gamma_2(\lambda'^2/\lambda) + \Gamma_3\lambda[\phi'^2 + (\theta'+1)^2\cos^2\phi + 3\cos^2\theta\cos^2\phi - 1] - u \tag{3}$$

where $(\,)' = \mathrm{d}/\mathrm{d}(\omega t)$ represents the nondimensional time derivative, $u = T/[(m_2 + m_t)L_f\omega^2]$ is the nondimensional control tension, T is the tether control tension, Q_θ and Q_ϕ are the generalized forces associated the distributed electromagnetic forces, λ is the nondimensional tether length normalized with respect to the fully deployed tether length L_f, ω is the orbit angular velocity, and

$$\Gamma_1 = \frac{m_2 + m_t/2}{m_2 + m_t/3}, \qquad \Gamma_2 = \frac{m_t}{2(m_2 + m_t)}, \qquad \Gamma_3 = \frac{m_2 + m_t/2}{m_2 + m_t} \tag{4}$$

are nondimensional mass parameters, where m_2 is the subsatellite mass and m_t is the tether mass, given by

$$m_t = \rho\lambda L_f \tag{5}$$

The generalized forces acting on the system can be evaluated in the following manner:

$$Q_{q_j} = \int_m \boldsymbol{F} \cdot \frac{\partial \boldsymbol{R}_m}{\partial q_j} \tag{6}$$

where $\boldsymbol{F}$ is the vector of external forces, $\boldsymbol{R}_m$ is the inertial vector to the line of action of the force $\boldsymbol{F}$ acting on the mth system mass, and q_j are the generalized coordinates. For the case of electromagnetic Lorentz forces, consider the force acting on a small element of the tether at a distance r from the center of mass (measured positively towards mass m_2). The elemental Lorentz force is given by

$$\mathrm{d}\boldsymbol{F} = I(r)(\boldsymbol{t} \times \boldsymbol{B})\,\mathrm{d}r \tag{7}$$

where $I(r)$ is the current in the tether at r, $\boldsymbol{t}$ is the unit vector tangent to the tether line in the direction of r, and $\boldsymbol{B}$ is the magnetic field vector measured at the center of mass of the system. It is assumed that the magnetic field is constant along the tether as in Ref. 42.

The calculation of the required vectors to evaluate the generalized forces is carried out in a rotating reference frame attached to the system center of mass. The unit vectors $\boldsymbol{i}, \boldsymbol{j}$, and $\boldsymbol{k}$ are introduced, which are aligned with the local vertical, local horizontal, and the orbit normal, respectively. The required vectors are given as follows:

$$\boldsymbol{t} = \cos\theta\cos\phi\boldsymbol{i} + \sin\theta\cos\phi\boldsymbol{j} + \sin\phi\boldsymbol{k} \tag{8}$$

$$\boldsymbol{R} = (R + r\cos\theta\cos\phi)\boldsymbol{i} + r\sin\theta\cos\phi\boldsymbol{j} + r\sin\phi\boldsymbol{k} \tag{9}$$

$$\boldsymbol{B} = B_x\boldsymbol{i} + B_y\boldsymbol{j} + B_z\boldsymbol{k} \tag{10}$$

The generalized forces can be evaluated as follows:

$$Q_{q_j} = \int_s^l \mathrm{d}\boldsymbol{F} \cdot \frac{\partial \boldsymbol{R}}{\partial q_j} = \int_s^l I(r)(\boldsymbol{t} \times \boldsymbol{B}) \cdot \frac{\partial \boldsymbol{R}}{\partial q_j}\,\mathrm{d}r \tag{11}$$

$$Q_\theta = \frac{I^* l^2}{2}\cos\phi[\sin\phi(B_x\cos\theta + B_y\sin\theta) - B_z\cos\phi] \tag{12}$$

$$Q_\phi = -\frac{I^* l^2}{2}(B_y\cos\theta - B_x\sin\theta) \tag{13}$$

where I^* is the average current defined by

$$I^* = \frac{2}{l^2}\int_0^l I(r)r \cdot \mathrm{d}r \tag{14}$$

Note that for a uniform current, $I^* = I$. In this paper, the effect of current distributions along the tether are ignored, and we treat I^* as the control variable. This assumption is a simplification and will need to be removed in future work, because the current distribution in a bare tether is not uniform.

B. Tether as a Continuum

A number of methods for modeling flexible tethers have been used in the literature. These can be divided into continuous and discrete models. One common approach for continuous models is to use a Galerkin-type expansion of the tether displacements into admissible coordinates. This approach has been used by Misra et al.[44] However, this approach becomes cumbersome for more than a few modes and can lead to numerical difficulties for high numbers of modes.[45] A common discretization approach is to model the tether as a series of point masses connected by massless elastic springs and dashpots. This approach has been used by the authors for simulating control laws and unscheduled tether operations[46] and has been used widely in the literature. In this paper, however, we employ a continuous model for the tether and mathematically discretize it using finite differences. This choice is made primarily on the insights that can be obtained from the form of the equations of motion.

Consider the material point located in the orbital frame $Oxyz$ (Fig. 1b), which is attached to the mother satellite, described by the vector

$$\boldsymbol{r}(s,t) = x(s,t)\boldsymbol{i} + y(s,t)\boldsymbol{j} + z(s,t)\boldsymbol{k} \tag{15}$$

where $s \in [0, L_f]$ is an arc length parameter describing the location of the undeformed material point, measured from the attachment point on the mother satellite, and t is time.

The partial differential equations governing the dynamics of the tether can be written as

$$\rho\frac{\partial^2 \boldsymbol{r}(s,t)}{\partial t^2} = -\rho\omega^2[-3x(s,t)\boldsymbol{i} + z(s,t)\boldsymbol{k}] - 2\rho\boldsymbol{\omega} \times \frac{\partial \boldsymbol{r}(s,t)}{\partial t} + \frac{\partial \boldsymbol{T}}{\partial s} + I(s)\frac{\partial \boldsymbol{r}(s,t)}{\partial s} \times \boldsymbol{B} \tag{16}$$

where ρ is the material density, $\boldsymbol{T}$ is the tether tension, I is the electric current flowing in the tether, $\boldsymbol{\omega} = \omega\boldsymbol{k}$ is the orbital angular velocity vector, and $\boldsymbol{B}$ is the magnetic field vector. Assuming that the tether tension is defined by Hooke's law and is everywhere tangent to the tether line, we have

$$\frac{\partial \boldsymbol{T}}{\partial s} = EA\left[1 - \frac{1}{\|\partial \boldsymbol{r}(s,t)/\partial s\|} + \frac{\partial \boldsymbol{r}(s,t)/\partial s \cdot \partial \boldsymbol{r}(s,t)/\partial s}{\|\partial \boldsymbol{r}(s,t)/\partial s\|^3}\right]\frac{\partial^2 \boldsymbol{r}(s,t)}{\partial s^2} \tag{17}$$

where EA is the tether longitudinal stiffness. Assuming that the point of attachment of the tether at the mother satellite is movable, $\boldsymbol{s}_0(t) = s_x(t)\boldsymbol{i} + s_y(t)\boldsymbol{j} + s_z(t)\boldsymbol{k}$, as shown in Fig. 2, the boundary conditions for Eq. (16) are

$$\boldsymbol{r}(0,t) = s_x(t)\boldsymbol{i} + s_y(t)\boldsymbol{j} + s_z(t)\boldsymbol{k} \tag{18}$$

$$m_2\frac{\partial^2 \boldsymbol{r}(L_f,t)}{\partial t^2} = -m_2\omega^2[-3x(L_f,t)\boldsymbol{i} + z(L_f,t)\boldsymbol{k}] - 2m_2\boldsymbol{\omega} \times \frac{\partial \boldsymbol{r}(L_f,t)}{\partial t} - T(L_f,t)\frac{\partial \boldsymbol{r}(L_f,t)}{\partial s} \tag{19}$$

The standard method for discretizing the equations of motion is to divide the arc length parameter outside the deployer into a constant number of elements via a finite difference method. This approach makes it difficult to solve the equations because the arc length parameter for each element varies with time. An alternative approach[47] is to divide the arc length parameter outside the deployer into a variable number of elements, $n = n(t)$. That is, the entire tether is divided into a constant number of elements N including the elements inside the deployer, as shown in Fig. 2. When the natural length of deployed tether exceeds a predetermined amount $h_n(t) > h^*$, the number of elements outside the deployer is increased. Conversely, when the natural length of deployed tether reduces below a predetermined amount, $h_n(t) < h^{**}$, an element is removed. This process is similar to that used in the bead models.[45] Special care must be taken in specifying the state vector for the new element. The position of a new element is determined by the continuity condition for tether tension in the new segment(s). The velocity for a new element is determined such that the component of velocity along the tether line at the attachment point is maintained, while the swing component of the velocity is reduced to maintain constant angular velocity of the tether at the attachment point.

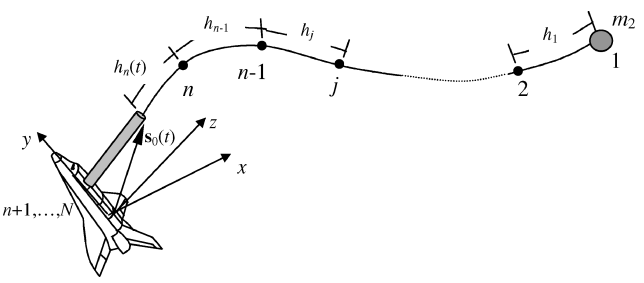

Fig. 2 Discretization of continuum tether model with movable attachment point.

C. Magnetic Field Vector

The Earth's magnetic field can be approximated as a dipole for preliminary analysis. The general equation for the magnetic field vector modelled by a dipole is given by[38]

$$\boldsymbol{B} = \left(\mu_m \big/ R^3\right)[\boldsymbol{u}_m - 3(\boldsymbol{u}_m \cdot \boldsymbol{u}_r)\boldsymbol{u}_r] \tag{20}$$

where $\boldsymbol{u}_m$ is the unit vector describing the orientation of the magnetic axis and $\boldsymbol{u}_r$ is the unit position vector of the point of interest where the magnetic field vector is to be determined. The magnetic field vector for a nontilted dipole in a circular orbit is as follows[39]:

$$B_x = -2\left(\mu_m \big/ R^3\right) \sin f \sin i \tag{21}$$

$$B_y = \left(\mu_m \big/ R^3\right) \cos f \sin i \tag{22}$$

$$B_z = \left(\mu_m \big/ R^3\right) \cos i \tag{23}$$

where μ_m is the dipole strength, R is the radius of the circular orbit, $f = \omega t$, and i is the orbit inclination.

III. Derivation of Control Laws

A. Libration Control Using Distributed Electric Current

The application of an electrical current in the tether generates Lorentz forces that are in a direction which is normal to both the tether line and the magnetic field vector. If it is assumed that the magnetic field vector is constant along the tether at any given instant and that the tether remains straight, then the Lorentz force will always be normal to the tether and constant in direction at each point. Therefore, by modulating the electric current at appropriate times it should be possible to control the tether librations.

In this paper, we consider combining both tension control and electromagnetic forces for controlling the librational motion of the system. The control law for the hybrid case can be derived by introducing the nondimensional mission function as

$$\mathcal{M} = \tfrac{1}{2}k_1(\lambda - \lambda_c)^2 + \tfrac{1}{2}\left(k_2 + \lambda^2\right)[\phi'^2 + 4\sin^2\phi + (\theta'^2 + 3\sin^2\theta)\cos^2\phi] + \tfrac{1}{2}k_4\lambda'^2 \tag{24}$$

where λ_c is the nondimensional tether length required to complete the mission, and k_1, k_2, and k_4 are control gains whose functions are described next. The mission function is based on the Hamiltonian for a massless tether.

The nondimensional time derivative of the mission function is

$$\begin{aligned}\mathcal{M}' = \lambda'\Big\{&k_1(\lambda - \lambda_c) - \lambda(1 - k_4\Gamma_3)[\phi'^2 + (\theta' + 1)^2\cos^2\phi \\ &+ 3\cos^2\theta\cos^2\phi - 1] + 3\lambda - k_4\Gamma_2(\lambda'^2/\lambda) \\ &- 2(k_2/\lambda)(\Gamma_1 + 1)[\phi'^2 + (\theta'^2 + \theta')\cos^2\phi] \\ &- 2\lambda\Gamma_1[\phi'^2 + (\theta'^2 + \theta')\cos^2\phi] - k_4 u\Big\} \\ &+ \left[I \big/ 2(m_2 + m_t/3)\omega^2\right]\left(k_2 + \lambda^2\right) \\ &\times [\theta'(\varepsilon_1 \sin\phi\cos\phi - \varepsilon_2) + \phi'\varepsilon_3]\end{aligned} \tag{25}$$

where $\varepsilon_1 = B_x\cos\theta + B_y\sin\theta$, $\varepsilon_2 = B_z\cos^2\phi$, $\varepsilon_3 = B_y\cos\theta - B_x\sin\theta$. Selection of the control inputs as

$$\begin{aligned}u = &(k_1/k_4)(\lambda - \lambda_c) - \lambda(1/k_4 - \Gamma_3)[\phi'^2 + (\theta' + 1)^2\cos^2\phi \\ &+ 3\cos^2\theta\cos^2\phi - 1] + 3\lambda/k_4 - \Gamma_2(\lambda'^2/\lambda) \\ &- 2(k_2/k_4\lambda)(\Gamma_1 + 1)[\phi'^2 + (\theta'^2 + \theta')\cos^2\phi] \\ &- 2(\lambda\Gamma_1/k_4)[\phi'^2 + (\theta'^2 + \theta')\cos^2\phi] + (k_3/k_4)\lambda'\end{aligned} \tag{26}$$

$$I = -2k_5(m_2 + m_t/3)\omega^2\left(k_2 + \lambda^2\right)[\theta'(\varepsilon_1\sin\phi\cos\phi - \varepsilon_2) + \phi'\varepsilon_3] \tag{27}$$

where k_3 and k_5 are additional control gains selected to ensure adequate control performance, gives a closed-loop nondimensional time derivative of the mission function of

$$\mathcal{M}' = -k_3\lambda'^2 - k_5\varphi^2 \tag{28}$$

where

$$\varphi = \left(k_2 + \lambda^2\right)[\theta'(\varepsilon_1\sin\phi\cos\phi - \varepsilon_2) + \phi'\varepsilon_3] \tag{29}$$

The selected controls give an asymptotically stable control law provided $k_3 > 0$ and $k_5 > 0$. The control gain k_5 regulates the amount of control current being applied to the tether. If the gain is set to $k_5 = 0$, then the control law utilizes tension only, and the electric current is zero. Also note that the formulation is independent of the form of the magnetic field vector and relies only on the instantaneous measurement of the magnetic field at the mother satellite.

The gain k_1 determines how quickly the length approaches the desired length λ_c, and the higher the value the more overshoot that can be expected. The gain k_2 primarily influences the damping of the out-of-plane librations and generally requires higher electric currents to be generated because of its presence in Eq. (27). There is also a greater variation in tether length and in-plane angle. The gain k_3 determines the amount of length variation and generally slows the damping of the out-of-plane librations. The gain k_4 determines how smooth the variation in tether length is. The gain k_5 determines the magnitude of the applied electric current. Note that there is a complicated interaction between the control gains, and they must be selected carefully to achieve the desired control of the dynamics.

It can be seen upon examination of Eqs. (28) and (29) that limitations do exist for the proposed control law. In particular, the time derivative of the mission function can be zero even with out-of-plane motion present because $\varepsilon_3 = 0$ for equatorial orbits and a nontilted magnetic dipole. In reality, the tilt of the dipole would allow some damping of the out-of-plane motion, even for zero inclination orbits, but this might not be very effective. The optimum situation, therefore, is when the tether system is on an inclined orbit so that components of the electromagnetic force will always exist to damp out-of-plane motion.

An important consideration in the analysis of utilizing electromagnetic forces as a control actuator is the generation of electric current within the tether. For a given system configuration there is a maximum allowable current that can be achieved. In general, this is a function of the ionospheric plasma density, magnetic field vector, and tether cross-sectional area. In this paper, some simplifying assumptions are made for the calculation of the maximum current. We assume a circular orbit of radius 6600 km and base the calculations on the ideal current generated using a bare wire anode,[48] with aluminum as the tether material. The ideal maximum current that can be generated is the short-circuit current

$$I_{\max} = E_m\sigma_t A_t \tag{30}$$

where $E_m = vB\cos i \approx 0.215\cos i$ V/m is the motional electric field along the tether, σ_t is the tether conductivity ($3.5 \times 10^7\ \Omega^{-1}\ \mathrm{m}^{-1}$ for aluminum), and A_t is the tether cross-sectional area. In this paper, we assume a tether diameter of 0.7 mm and limit the allowable current to 1.75 A in all calculations. This is a reasonable value based on the orbit inclination, $i = 51.2$ deg, studied throughout the paper. Note that future work should be undertaken to include the full interaction of a bare tether with variations in the ionospheric plasma, as well as the impact of the variation of the electric current along the tether length.

B. Wave-Absorbing Control

Electromagnetic forces are always perpendicular to the tether line, and this can cause significant lateral deflections of the tether. The combined variation in the magnetic field and tether current caused by the control law means that high-order vibratory modes

are likely to be initiated. These modes were not taken into account in the derivation of the control law for the electric current, and some method must be introduced to account for these effects.

Consideration was given to formulating the current control law based on a flexible tether model. This would require measurement and feedback of the dynamical state of the tether and would be impractical. In this paper, we assume that the sensory input comes only from measurements of the tether state at the deployer and the motion of the subsatellite. Therefore, a technique that utilizes the boundary conditions of the system appears to be the most appropriate approach.

Wave-absorbing control of large space structures has been studied by Von Flotow[49] and Fujii and Colleagues.[50–52] This approach views the vibrational response of a structure to consist of traveling elastic disturbances. The traveling waves can be related mathematically as incoming and outgoing wave vectors at controller positions. By appropriate choice of control input, it is possible to obtain relationships between incoming and outgoing waves to provide closed-loop control of the wave disturbances. Fujii et al.[53] have specifically used such a technique to control the in-plane transverse motion of tethered systems. In this section, we extend the previous work presented in Ref. 53 to the case of in- and out-of-plane motion in the presence of electromagnetic forces.

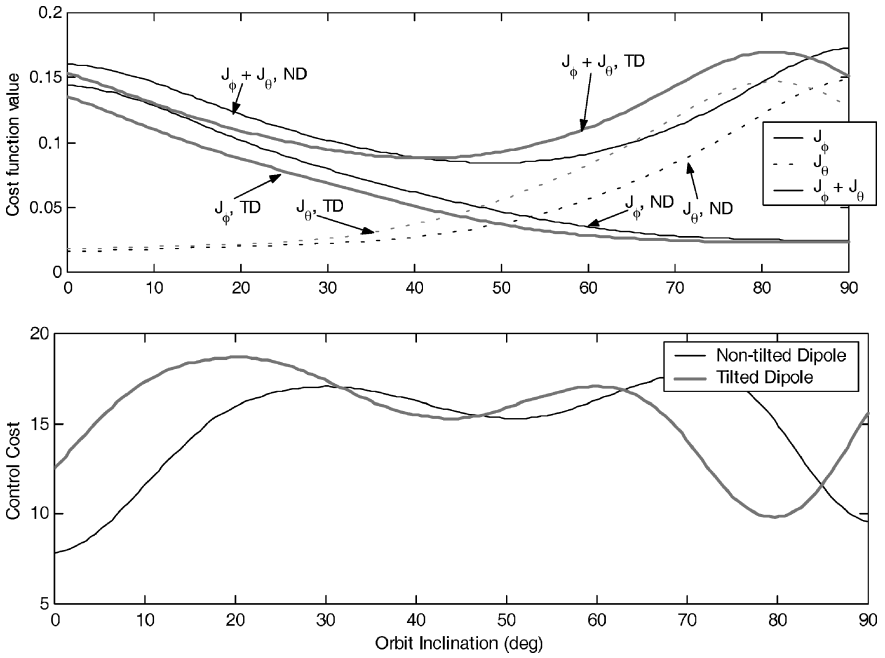

Fig. 3 Study on the effectiveness of libration control using electromagnetic forces for nontilted and tilted dipole cases (top to bottom): a) variations in cost functions J_ϕ, J_θ, and $J_{\phi,\theta}$ for inclinations $0 \le i \le 90$ deg and b) variation in cost function J_I for inclination $0 \le i \le 90$ deg (ND = nontilted dipole, TD = tilted dipole).

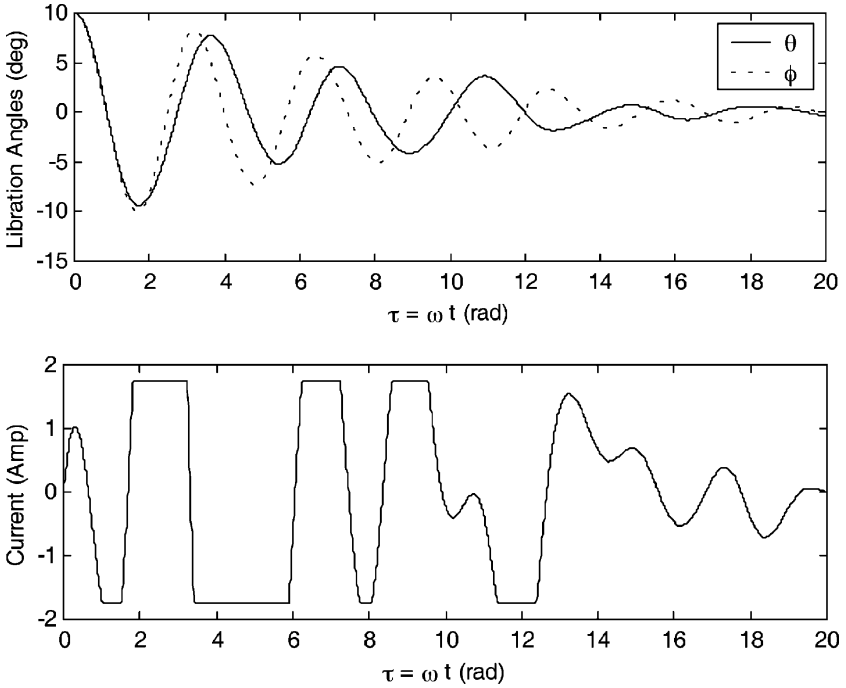

Fig. 4 Control of tether librations via electromagnetic forces for a nontilted dipole and orbit inclination, i = 51.2 deg (top to bottom): a) in- and out-of-plane librations and b) control current.

The governing equations of motion for the tether in Cartesian coordinates, ignoring electromagnetic forces, are given by

$$\rho\frac{\partial^2 x}{\partial t^2}=\frac{\partial}{\partial s}\left(T\frac{\partial x}{\partial s}\right)+3\omega^2 x+2\frac{\partial y}{\partial t}\omega$$

$$\rho\frac{\partial^2 y}{\partial t^2}=\frac{\partial}{\partial s}\left(T\frac{\partial y}{\partial s}\right)-2\frac{\partial x}{\partial t}\omega,\qquad \rho\frac{\partial^2 z}{\partial t^2}=\frac{\partial}{\partial s}\left(T\frac{\partial z}{\partial s}\right)-z\omega^2 \tag{31}$$

Restricting attention to transverse displacements superimposed on the rigid-body tether modes leads to the equation governing the transverse motion:

$$\rho\frac{\partial^2 w}{\partial t^2}=\frac{\partial}{\partial s}\left(T\frac{\partial w}{\partial s}\right) \tag{32}$$

where $w\in[y,z]$. In general, the tether tension varies with time, either through a controller or because of librations, and with position s along the tether. In cases where $m_2\gg m_t$, which is satisfied for the cases studied in this paper, the variation in tension along the tether can be neglected, and Eq. (32) reduces to the wave equation

$$\rho\frac{\partial^2 w(s,t)}{\partial t^2}=T\frac{\partial^2 w(s,t)}{\partial s^2} \tag{33}$$

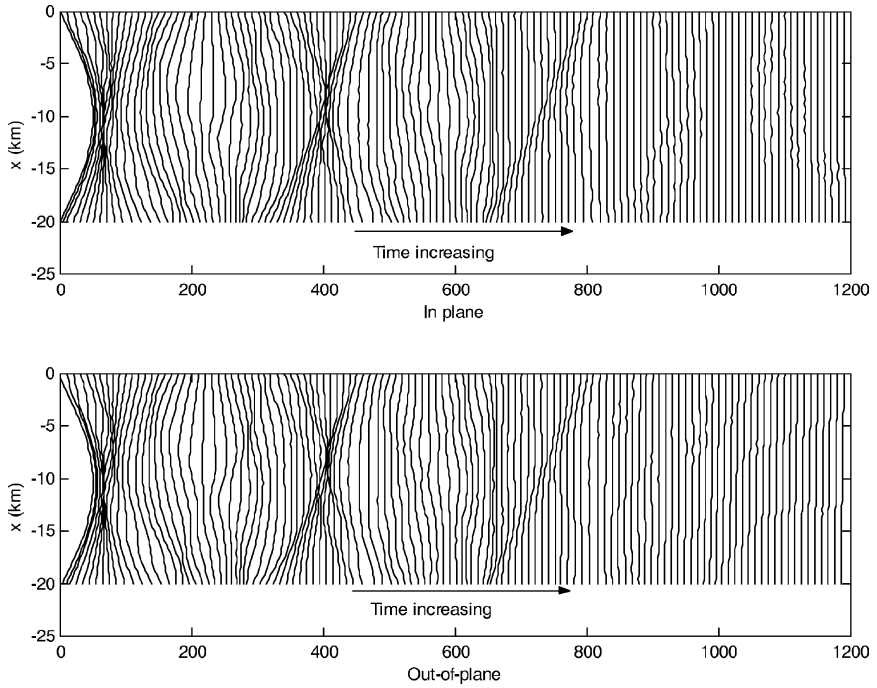

Fig. 5 Wave-absorbing control of in- and out-of-plane transverse traveling waves by movement of the tether attachment point (simulation time is 1200 s, snapshots are at 8-s intervals) (top to bottom): a) in plane and b) out of plane.

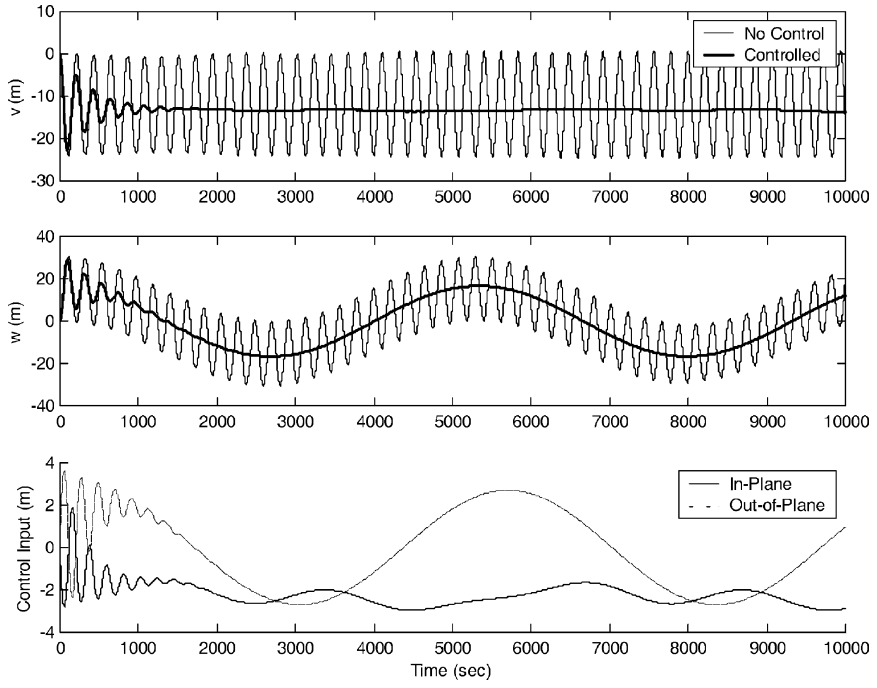

Fig. 6 Control of tranverse motion of electromagnetic tether under constant current (I = 0.5 A) with wave-absorbing control (K = 50) (top to bottom): a) in-plane deflection of tether midpoint, b) out-of-plane deflection of tether midpoint, and c) displacement of tether attachment point.

For the cases studied in this paper, the frequencies of the transverse oscillations of the tether are higher than changes in the tether tension caused by librations or control requirements, and hence T can be taken to be quasi-steady in Eq. (33) when taking the Laplace transform

$$\rho\bar{s}^2 w(s,\bar{s}) = T\frac{\partial^2 w(s,\bar{s})}{\partial s^2} \Rightarrow \frac{\partial^2 w(s,\bar{s})}{\partial s^2} - \frac{\bar{s}^2}{c^2}w(s,\bar{s}) = 0 \quad (34)$$

where $\bar{s}$ is the Laplace variable, and $c = \sqrt{(T/\rho)}$ = speed of traveling wave. The general solution to Eq. (34) is given by

$$w(s,\bar{s}) = Ae^{s\bar{s}/c} + Be^{-s\bar{s}/c} \quad (35)$$

where A and B are the amplitudes of the incoming and outgoing waves, respectively. If the control actuator at $s = 0$ is selected to be implemented via the velocity of the attachment point, then the selection of the control law as

$$\frac{\partial w(0,t)}{\partial t} = K\frac{\partial w(0,t)}{\partial s} \quad (36)$$

allows the relationship of the outgoing and incoming wave amplitudes to be determined as

$$B/A = [K - c]/[K + c] \quad (37)$$

From Eq. (37) it can be seen that the optimum control gain for decreasing the amplitude of the outgoing waves, thereby absorbing the energy from the incoming waves, is $K = c = \sqrt{(T/\rho)}$. However, in most practical tether systems moving the attachment point will be limited by the maximum allowable displacement of the system. Therefore limitations must be placed on the control gain as follows:

$$K = \begin{cases} 0 & \text{if} \quad w(0,t) \geq w_{\max} \\ c & \text{if} \quad w_{\min} < w(0,t) < w_{\max} \\ 0 & \text{if} \quad w(0,t) \leq w_{\min} \end{cases} \quad (38)$$

In the case where the control input is saturated, the outgoing waves will remain at the same amplitude as the incoming waves, as shown in Eq. (37).

For wave-absorbing control of a tether with electric current present, the control law needs to be modified from its present form

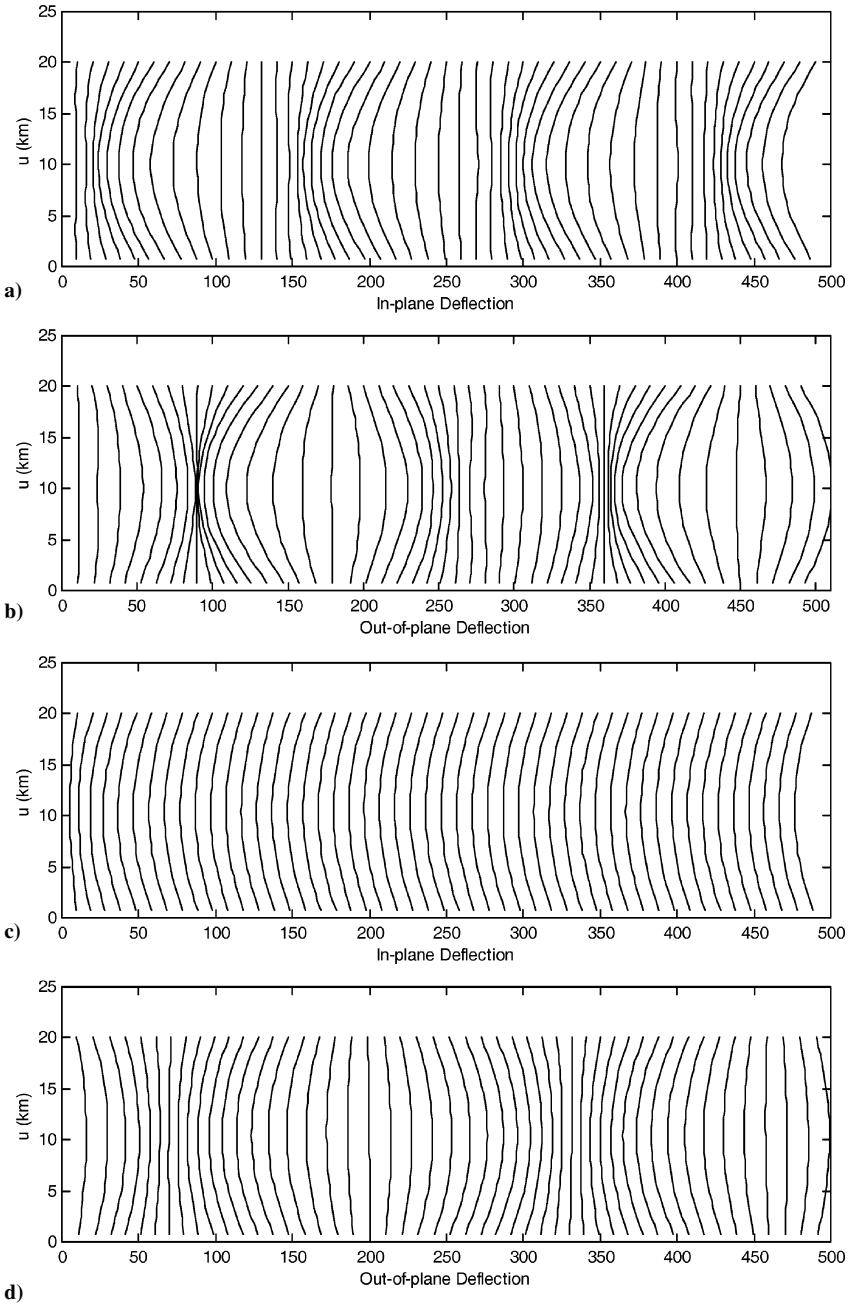

Fig. 7 Projections of tether deflection under constant current (I = 0.5 A) with a), b) no wave-absorbing control and c), d) wave-absorbing control (taken every 200 s) (top to bottom): a), c) in-plane deflection and b), d) out-of-plane deflection.

because of the transverse loading on the tether. In this paper, some ideal assumptions are adopted to derive the modification to the control law. At any instant of time, there can be considered to be a tether shape whereby the external loading on the tether is balanced by the internal tension forces. The transverse traveling waves can be considered to be superimposed on this deflection. To estimate this shape for an electromagnetic tether, it is assumed, first, that the bending of the tether occurs at constant tension equal to the tension induced by librations or by the tension control system. Second, the transverse loading is assumed to be constant along the length, and its value is based on the undeformed tether shape. Under these assumptions, the wave-absorbing control law becomes

$$\frac{\partial w(0,t)}{\partial t} = K\left[\frac{\partial w(0,t)}{\partial s} - \sin^{-1}\left(\frac{F_w}{2T_0}\right)\right] \tag{39}$$

where T_0 is the tether control tension, or when no active tension control is used, is given by Eq. (40), and F_w is the electromagnetic force on the tether in the in- (y) and out-of-plane (z) directions, given by Eqs. (41) and (42), respectively.

$$T_0 = (m_2 + m_t/2)\omega^2 l[\phi'^2 + (\theta' + 1)^2\cos^2\phi + 3\cos^2\theta\cos^2\phi - 1] \tag{40}$$

$$F_y = Il(B_x\cos\theta\sin\phi + B_y\sin\theta\sin\phi + B_z\cos\phi) \tag{41}$$

$$F_z = Il(B_x\sin\theta - B_y\cos\theta) \tag{42}$$

Note that the wave-absorbing control law, Eq. (39), can be applied to different types of external loadings if estimates of the tether angle at the attachment point arising from such loadings can be made, such as those caused by aerodynamic drag or current variations along the tether.

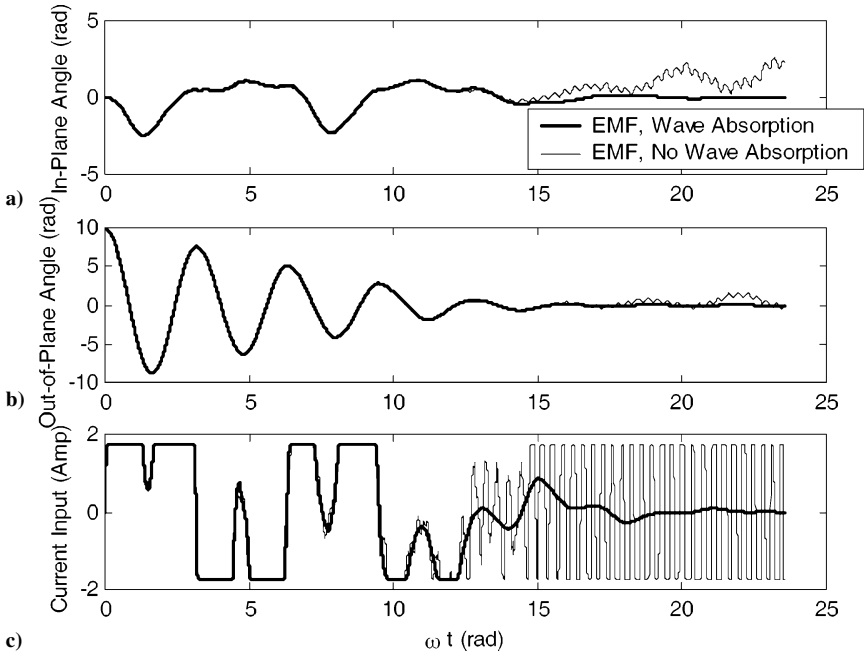

Fig. 8 Libration control using electromagnetic forces and wave-absorbing control (top to bottom): a) in-plane libration angle, b) out-of-plane libration angle, and c) control current.

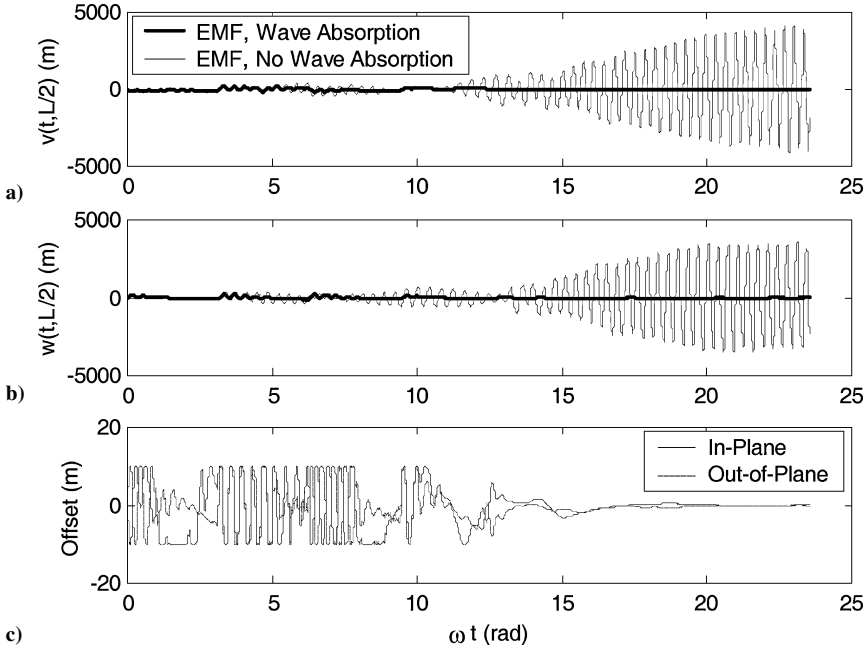

Fig. 9 Libration control using electromagnetic forces and wave-absorbing control (top to bottom): a) in-plane deflection of tether midpoint, b) out-of-plane deflection of tether midpoint, and c) attachment point control input.

Table 1 Simulation parameters[a]

Parameter	Case 1	Case 2	Case 3
Tether length L_f	20 km	20 km	20 km
Subsatellite mass m_2	200 kg	200 kg	200 kg
Tether density ρ	1 kg/km	1 kg/km	1 kg/km
Orbit semimajor axis a	6,600 km	6,600 km	6,600 km
Orbit inclination	——	51.2 deg	51.2 deg
Initial conditions $\{\theta_0, \theta_0', \phi_0, \phi_0', \lambda_0, \lambda_0'\}$	{10 deg, 0, 10 deg, 0, 1, 0}	{0, 0, 10 deg, 0, 1, 0}	Dep.: {0 deg, 0, 30 deg, 0, 0.02, 15 m/s} Ret.:{0, 0, 15 deg, 0, 1, 0}
Maximum allowable current $\|I\|_{\max}$	1.75 A	1.75 A	1.75 A
k_1, k_2, k_3, k_4, k_5	0, 0, 0, 0, 2e9	0, 0, 0, 0, 2e9	Dep.: 1, 0, 4, 0.5, 2e9 Ret.: 0.95, 1.5, 3, 2.5, 2e9
Tether stiffness EA	——	40,000 N	40,000 N
Discretisation	——	45 elements	45 elements
Wave-absorbing control Gain K	——	$\|I\| < 1.0$, 50; $\|I\| \geq 1.0$, $50/\|I\|$	$\|I\| < 1.0$, 50; $\|I\| \geq 1.0$, $50/\|I\|$
Maximum offset displacement	——	10 m	10 m
Tilted-dipole case			
Date at start of simulations	1200 h, 1 Jan. 2003	——	——
Longitude of ascending node	0	——	——

[a]Case 1: Study on effectiveness of EMF control with orbit inclination (simulation time = 20 radians); case 2: libration control using combined EMF and wave-absorbing controller (stationkeeping); case 3: deployment/retrieval simulations using combined EMF, tension, and wave-absorbing controller.

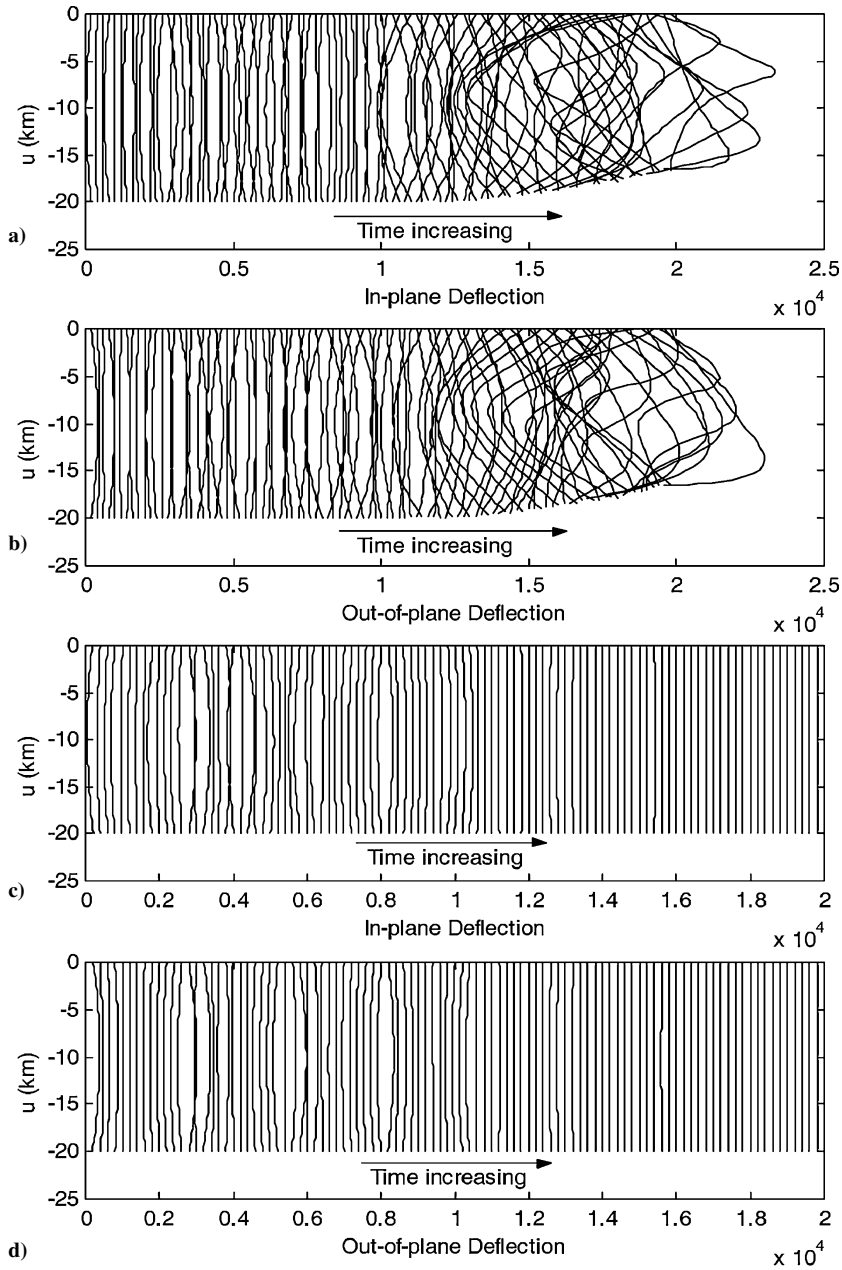

Fig. 10 Libration control using electromagnetic forces and a), b) no wave-absorbing control and c), d) with wave-absorbing control (top to bottom): a), c) In-plane tether deflection and b), d) out-of-plane tether deflection.

IV. Numerical Results

A. Current Control of Librations with Fixed Length Rigid Tether

An initial study was conducted to determine the orbit inclination that offers the optimum means for damping tether librations via electromagnetic forces. A polar orbit naturally offers maximum damping capability for out-of-plane librations, but no ability to control in-plane librations (for a nontilted dipole). This is not a major drawback because the in-plane librations can be controlled adequately via tension control. Conversely, an equatorial orbit offers the maximum damping capability for in-plane librations but none for out of plane. Therefore, there is a compromise between damping in- and out-of-plane librations. Furthermore, it is important to consider the requirements on the controller, because mathematically arbitrarily large electromagnetic forces can be generated. The study conducted in this paper restricts the maximum allowable current and employs the following cost functions for comparison

$$J_\phi = \frac{1}{2}\int_{t_0}^{t_f} \phi^2 \, \mathrm{d}t \tag{43}$$

$$J_\theta = \frac{1}{2}\int_{t_0}^{t_f} \theta^2 \, \mathrm{d}t \tag{44}$$

$$J_{\phi,\theta} = \frac{1}{2}\int_{t_0}^{t_f} (\phi^2 + \theta^2) \, \mathrm{d}t = J_\phi + J_\theta \tag{45}$$

$$J_I = \frac{1}{2}\int_{t_0}^{t_f} I^2 \, \mathrm{d}t \tag{46}$$

The parameters used for the study are given in Table 1, case 1. Note that the selected initial conditions and simulation time are arbitrary. The results from the study are summarized in Fig. 3, which shows the variations in cost function with orbit inclination for nontilted and tilted dipole cases. Figure 3a shows the variations in cost functions defined in Eqs. (43–45) for both tilted and nontilted dipole cases. It can be seen that when considering the combined control of both in- and out-of-plane librations that there is an ideal inclination for the system at approximately 50 deg. In addition, in this region of inclinations a local minimum in the control effort is observed, as shown in Fig. 3b. This local minimum occurs at approximately 51.2-deg inclination for a nontilted dipole. The dynamics of the system for the case of 51.2-deg inclination and a nontilted dipole is shown in Fig. 4. The overall characteristics of the costs are not substantially different for the two dipole cases. The general behavior of the tilted dipole case, however, varies with the time of day and orientation of the orbit with respect to the Earth as a result of the effect of the Earth's rotation. However, in spite of such variations, the control law is still effective in its ability to control the tether librations. For the remainder of this paper, the nontilted dipole model is utilized.

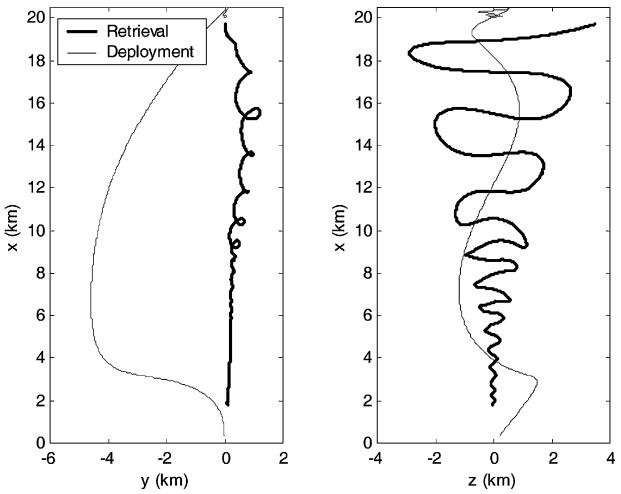

Fig. 12 Deployment/retrieval paths of the subsatellite on rigid tether using mission function control algorithm with tension and electromagnetic forces (left to right): a) in-plane path and b) out-of-plane path.

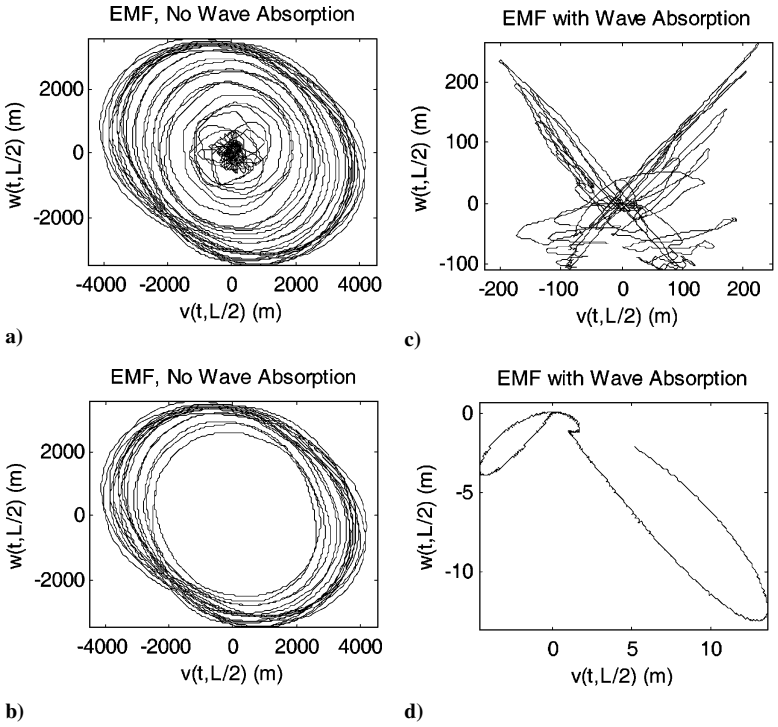

Fig. 11 Libration control using electromagnetic forces and wave-absorbing control (top to bottom): a) trajectory of tether midpoint with no wave absorption, b) trajectory of tether midpoint with no wave absorption ($17.6 < \omega t < 23.6$), c) trajectory of tether midpoint with wave absorption, and d) trajectory of tether midpoint with wave absorption ($17.6 < \omega t < 23.6$).

B. Traveling Wave Absorption by Moving the Attachment Point

1. Absorption of Traveling Waves in Absence of External Forces

The feasibility of using the tether attachment point to absorb in- and out-of-plane traveling waves on the tether is illustrated in Fig. 5 for the case where $K = c$. The numerical simulation was performed with initial conditions with the first transverse mode initiated in the in- and out-of-plane directions with an amplitude of 50 m. The tether properties are taken from Table 1 (case 2), while the maximum displacement of the attachment point is limited to 10 m. These results show that it is possible to damp the traveling wave in under 20 min.

2. Stabilization of EMF Tether Under Constant Current

To demonstrate the effect of wave-absorbing control for electromagnetic forces, we first consider the case of a constant current. Such a case has practical interest in applications such as electrodynamic reboost or deorbit applications. It has been noted[54] that electrodynamic tethers tend to be unstable when under a constant current. It is worthwhile to illustrate the stabilization that can be obtained by utilizing the proposed wave-absorbing control scheme. The case of a constant 0.5 A current is performed for the same case as earlier (properties in Table 1, case 2), but with the tether initially straight, and aligned with the

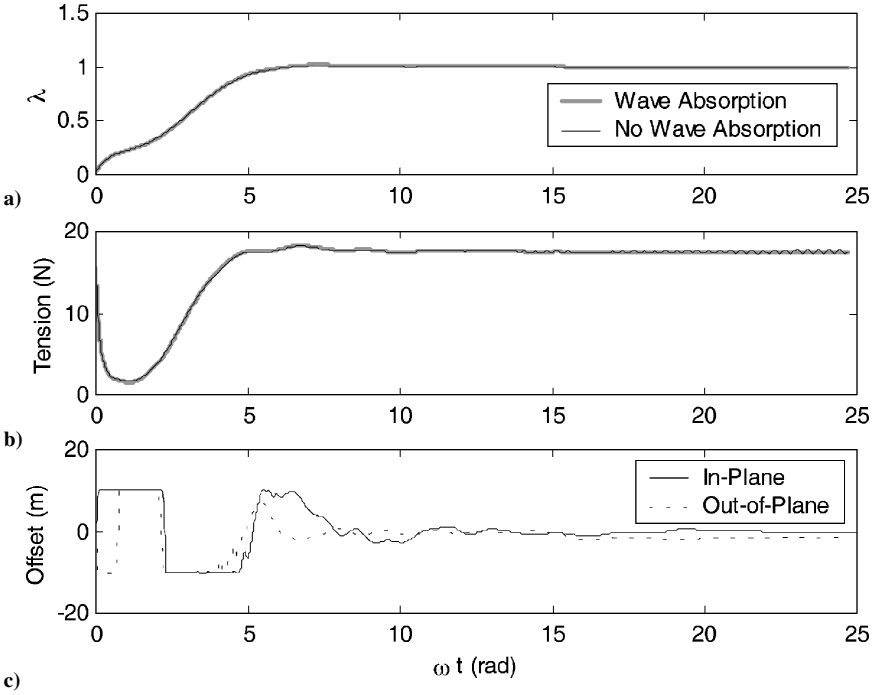

Fig. 13 Deployment simulation results using mission function control algorithm with tension and electromagnetic forces and flexible tether (top to bottom): a) nondimensional tether length, b) tether control tension, and c) attachment point.

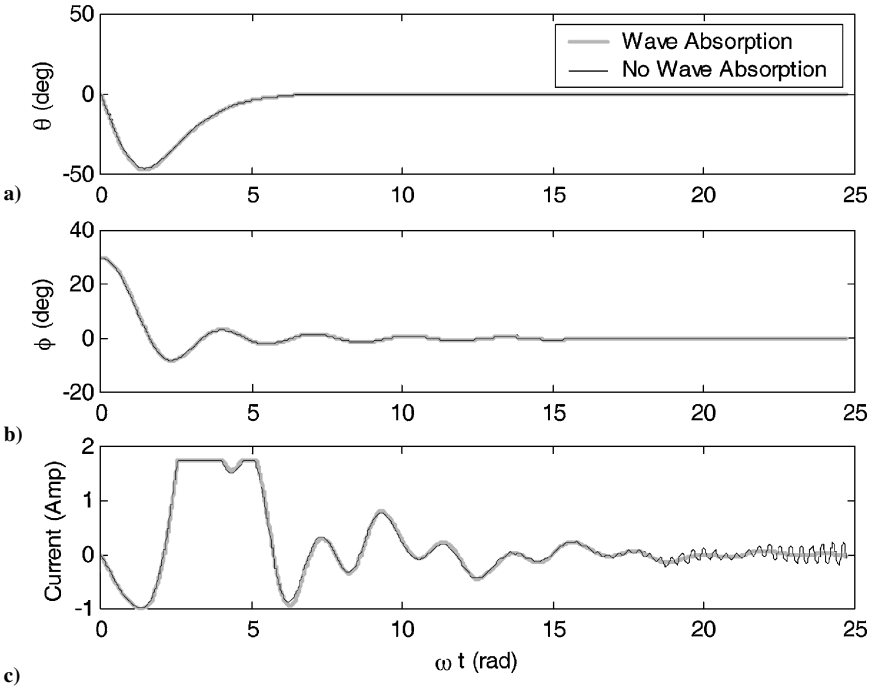

Fig. 14 Deployment simulation results using mission function control algorithm with tension and electromagnetic forces and flexible tether (top to bottom): a), b) in- and out-of-plane libration angles and c) control current.

local vertical. In addition, the control gain is selected to be constant $K = 50$.

Figures 6 and 7 illustrate the effect of wave absorption on the transverse motion of an electrodynamic tether under a constant current. It is observed that the sudden application of a constant current to the tether causes the tether to oscillate laterally. Figure 6 shows that the in-plane deflection of the midpoint of the tether is growing gradually, whereas the out-of-plane deflection varies with two frequencies and amplitudes. The first frequency is the mode of vibration initiated by application of electromagnetic (EM) forces at the beginning of the simulation. The low-frequency deflection coincides with the variation in direction of the out-of-plane force component on the tether during an orbit. The wave-absorbing controller is able to damp the transverse oscillations of the tether in approximately 20 min with only moderate movement of the tether attachment point. Figure 7 shows that the tether achieves a near steady-state in-plane deflection caused by the EM forces.

3. Combined Offset and Electromagnetic Control of Flexible Tether During Stationkeeping

We consider the case where the combined actuation of the tether is performed using both electromagnetics and wave-absorbing control. The parameters used in this simulation are given in Table 1, case 2. For simplicity, no changes in tether length are assumed, but an out-of-plane displacement of 10 deg is considered. Results from simulations with and without wave absorption are shown in Figs. 8–11. Figure 8 shows the librational motion of the system in response to the mission function control using electromagnetic forces. The in- and out-of-plane motion can be seen to be stabilized by the electromagnetic forces, and results from both cases agree well until

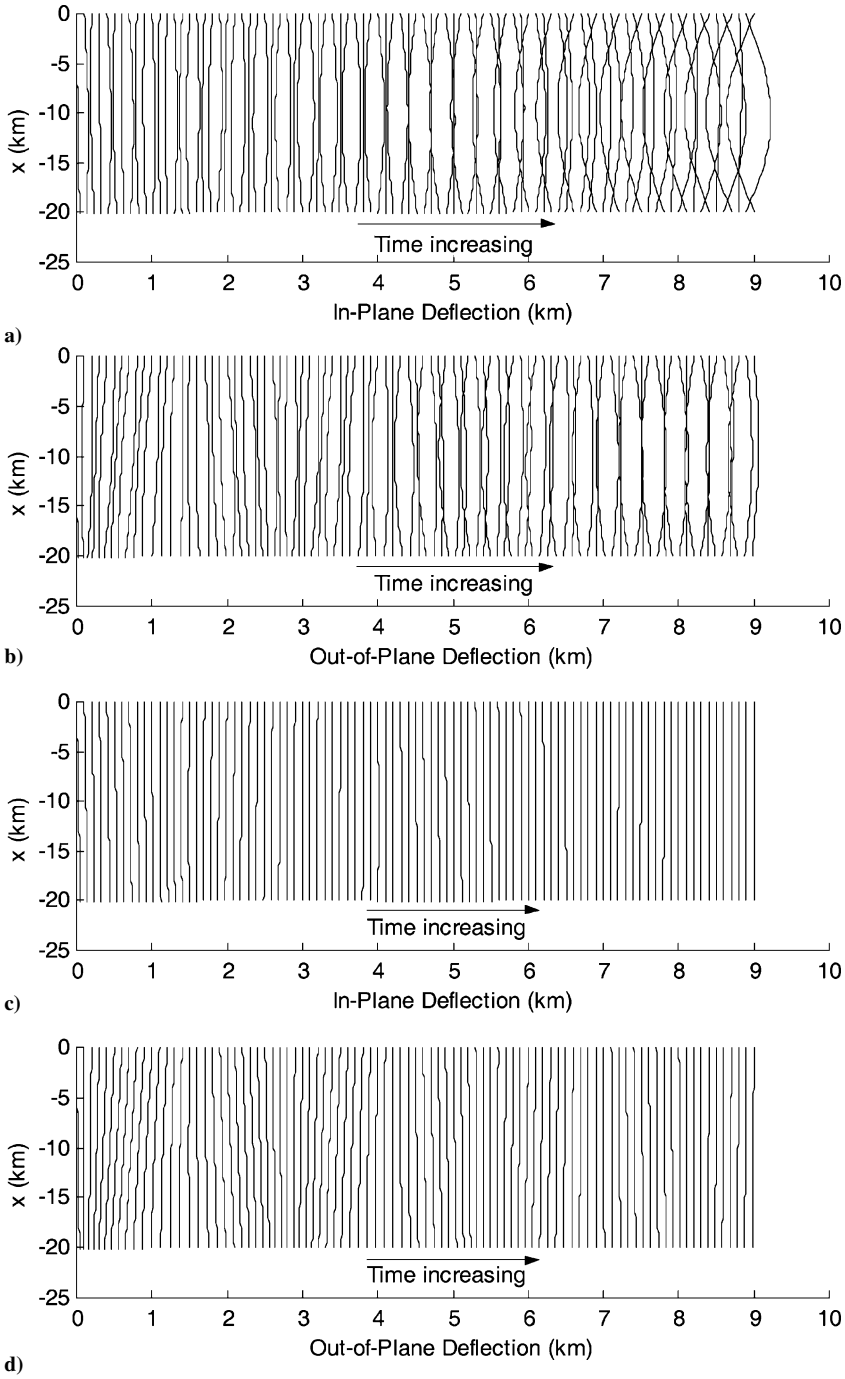

Fig. 15 Projections of tether deflections caused by electromagnetic forces following deployment ($14.1 < \omega t < 24.7$; plotted at intervals 0.12 rad) and a), b) no wave-absorbing control, c), d) with wave-absorbing control (top to bottom): a), c) in-plane deflection and b), d) out-of-plane deflection.

approximately 13 rad, where the case without wave absorption becomes unstable. This is a result of the instability in the transverse motion of the tether in the absence of wave-absorbing control, as can be seen clearly in Figs. 9 and 10. The amplitude of the transverse displacement reaches approximately 4 km in the in-plane direction by the end of the simulation, and this appears to be growing, as shown in the trajectory plot in Fig. 11. In fact, Figs. 11a and 11b show that the tether has gone into an unstable skip-rope motion. In contrast, the case where wave absorption is included shows that the transverse oscillations are extremely well suppressed. Figures 9 and 11d show that the wave-absorbing controller has almost completely eliminated the transverse instabilities, and the tether does not show any signs of skip-rope motion. The offset control required to achieve this result is shown in Fig. 9c. This illustrates that the controller saturates at a number of points, corresponding to the large current being applied at the beginning of the simulation. As the current decreases, however, the offset control correspondingly reduces. These results clearly establish the excellent performance of the wave-absorbing controller for damping the transverse motion of the tether system.

C. Combined Tension, Current, and Offset Control with Variable Length Tether

1. *Deployment*

In this section we consider the deployment of a 20-km tether using electromagnetics to damp the librational motion of the tether. The parameters used for the simulation are shown in Table 1, case 3.

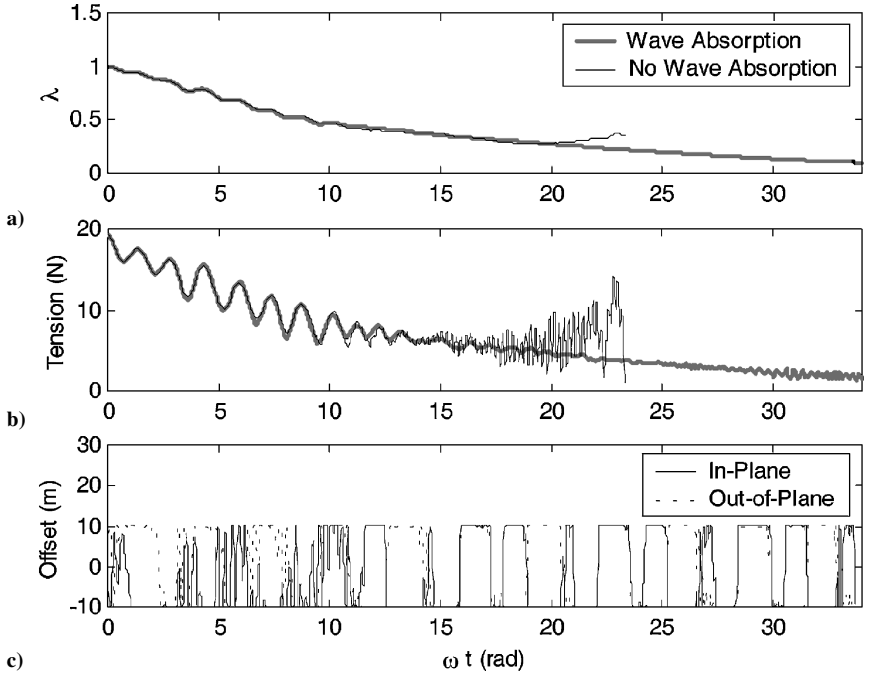

Fig. 16 Retrieval simulation results using mission function control algorithm with tension and electromagnetic forces and flexible tether (top to bottom): a) nondimensional tether length, b) tether control tension, and c) attachment point.

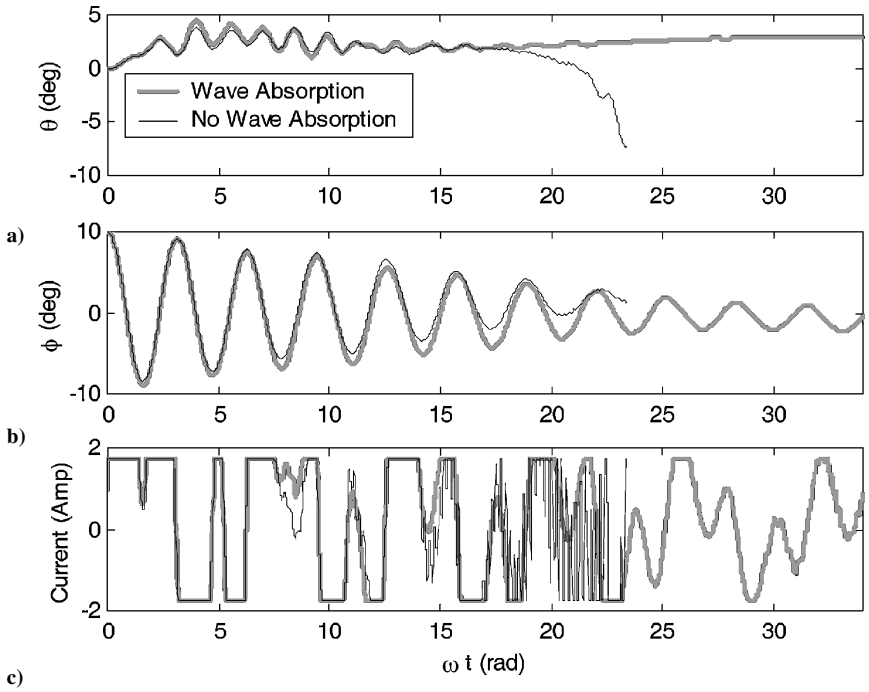

Fig. 17 Retrieval simulation results using mission function control algorithm with tension and electromagnetic forces and flexible tether (top to bottom): a) in-plane libration angle, b) out-of-plane libration angles, and c) control current.

The mission function control algorithm requires appropriate selection of the control gains to ensure adequate performance of the controller. The mission objective is to deploy the tether from 0.4 to 20 km along the local vertical. Numerical simulation results are shown in Figs. 12–15. Figure 12 shows the deployment path of the subsatellite in the in- and out-of-plane directions. Figures 13 and 14 show the dynamics of the system during and after deployment. It can be observed that the combination of electromagnetic and tension control is very effective at suppressing the in- and out-of-plane librational motion. The required current control, shown in Fig. 14c, illustrates that only moderate currents are required to damp the out-of-plane librations. This is a result of the inherent stability of the deployment phase. Figures 13–15 also illustrate the effect of the wave-absorbing controller. If no wave absorption is used, then the lateral modes begin to grow unstable at the end of deployment, as shown in Figs. 15a and 15b. However, when the wave-absorbing controller is used the tether remains basically straight, as shown in Figs. 15c and 15d. The required movement of the attachment point is shown in Fig. 13c. It can be noted, however, that the librational dynamics of the system are virtually identical whether wave absorption is used or not.

2. *Retrieval*

The effect of tether flexibility is nontrivial, particularly during retrieval. Kim and Vadali[45] demonstrate that the tether tends to commence skip-rope motion during retrieval if it is excited by an external force in the out-of-plane transverse direction. The inherent instability of the tether during retrieval suggests that using electromagnetic forces as a control actuator might not be wise during the retrieval phase. However, it might be possible to limit the instability by proper use of the wave-absorbing controller. Simulation results, using the numerical parameters from Table 1, case 3 are shown in

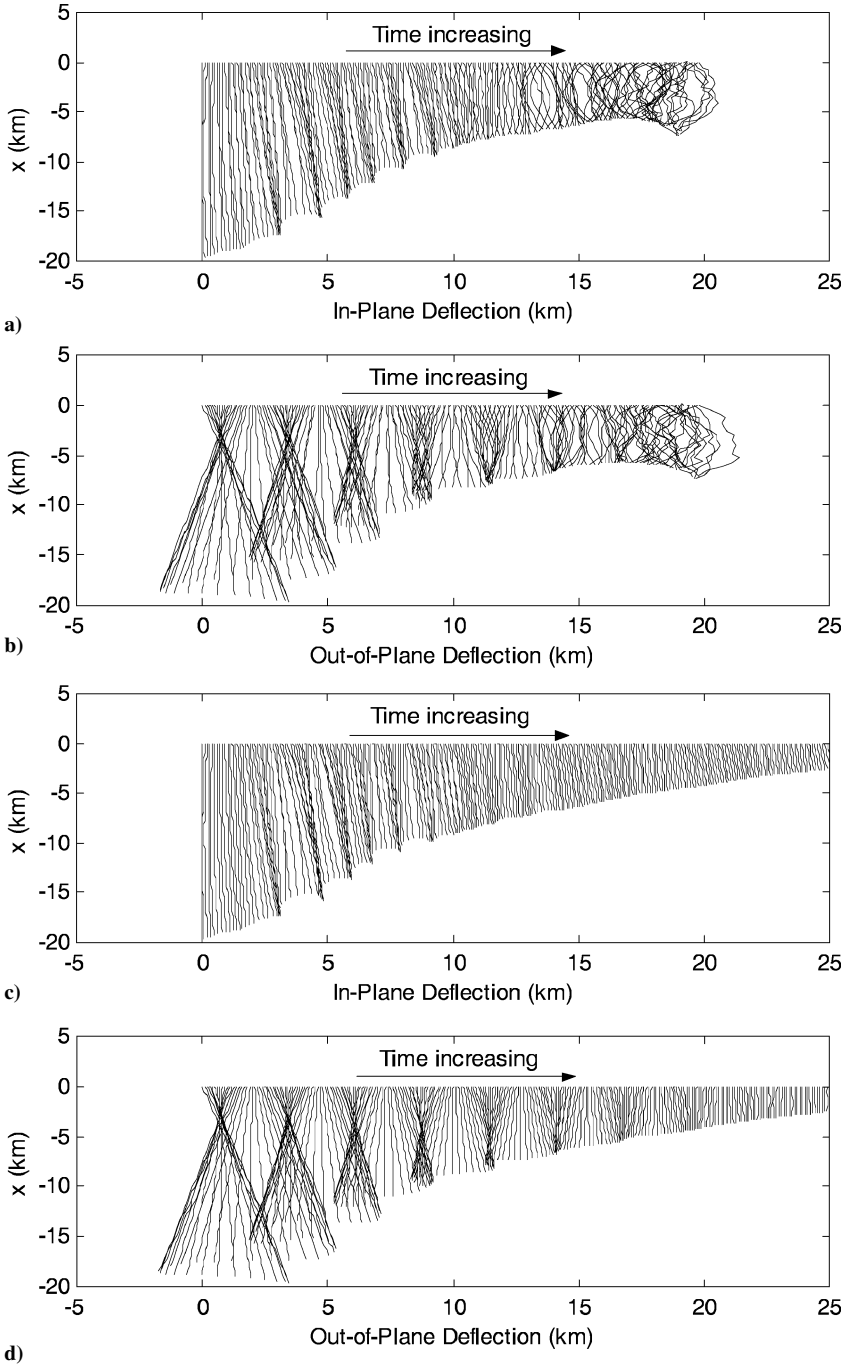

Fig. 18 Projections of tether deflections caused by electromagnetic forces during retrieval and a), b) no wave-absorbing control and c), d) with wave-absorbing control (top to bottom): a), c) in-plane deflection and b), d) out-of-plane deflection.

Figs. 12 and 16–18. Figure 12 shows the retrieval path in the in- and out-of-plane directions. This illustrates that the in- and out-of-plane displacements remain stable during retrieval under tension and electromagnetic control. Figures 16–18 compare the same retrieval scenario with and without wave absorption. It is evident that when no wave absorption is used the dynamics are dramatically influenced by the transverse displacements. The retrieval dynamics are similar with and without wave absorption until approximately 12 radians after the commencement of retrieval. At this point the tension and current control inputs begin to oscillate, and there is a loss of control. The transverse displacements become wild, as shown in the projections in Fig. 18. However, when wave absorption is used, the retrieval dynamics behave in a much more desirable manner. The tether tension and current input remain stable when the transverse displacements are adequately suppressed. This also causes the librational dynamics to behave excellently, particularly towards the end of the simulation. Projections of the tether shape during retrieval are shown in Figs. 18c and 18d. where the lateral instabilities can be seen to be suppressed by proper movement of the tether attachment point. The required movement of the attachment point to suppress the transverse displacements during retrieval is shown in Fig. 16c. It can be observed that the attachment point movement is essentially bang-bang for the entire retrieval phase. This clearly illustrates the need to employ a control actuator for suppressing the transverse displacements of the tether during retrieval with electromagnetic forces.

V. Conclusions

This paper has studied the use of electromagnetic Lorentz forces as a control actuator for controlling the librational dynamics of a tethered system. It has been demonstrated that it is possible to vary the current in the tether so that both in- and out-of-plane librations can be damped. A nonlinear hybrid control law was derived using Lyapunov's second method that combines tether tension control with current control. The control is asymptotically stable in a low-order model of the system dynamics, but can lead to instability in the lateral modes when tether flexibility and elasticity is accounted for. The lateral instability can be mitigated by the application of a wave-absorbing control scheme, which employs movement of the tether attachment point. Numerical simulation results clearly demonstrate the ability of the wave-absorbing controller to damp the lateral tether modes, even in the presence of large electromagnetic forces.

Several assumptions have been employed throughout the analysis that limit the application of the proposed control laws. In particular, it has been assumed that the electric current is used completely as a control input for damping the librational motion. This limits the current control law to nonelectrodynamic tethers such as those used in SEDS-I and II. Future work should include evaluating the performance of electromagnetic forces for librational tracking control in applications such as payload transfer. More advanced control methodologies, such as those based on optimal control, would be needed for this purpose. Further analysis on the costs of a system using electromagnetics as opposed to thrusters should also be undertaken to assess the practicality of using such a system for long-term applications. For nonelectrodynamic tethers, the complexity of the system by adding plasma contactors and other additional hardware could offset the advantages of using the system. Finally, application of the control schemes for electrodynamic tethers, such as that used during the TSS-1R mission, should be investigated. In these systems electric current is present and related to the mission, such as to avoid short circuits during deployment and retrieval (TSS-1R). In this scenario, the possibility of controlling the system by superimposing a control current over the mission current should be studied, as well as the associated costs.

Acknowledgments

The authors thank the anonymous reviewers for their invaluable comments on the draft of this paper. Their suggestions considerably improved the final version of the manuscript.

References

[1]Colombo, G., Gaposchkin, E. M., Grossi, M. D., and Weiffenbach, G. C., "The 'Sky-hook': A Shuttle-Borne Tool for Low-Orbital-Altitude Research," *Meccanica*, Vol. 10, March 1975, pp. 3–20.

[2]Kalaghan, P. M., Arnold, D. A., Colombo, G., Grossi, M. D., Kirschner, L. R., and Orringer, O., "Study of the Dynamics of a Tethered Satellite System (Skyhook)," Smithsonian Inst. Astrophysical Observatory, Final Report Contract NAS8-32199, Cambridge, MA, March 1978.

[3]Kyroudis, G. A., and Conway, B. A., "Advantages of Tether Release of Satellites from Elliptic Orbits," *Journal of Guidance, Control, and Dynamics*, Vol. 11, No. 5, 1988, pp. 441–448.

[4]Bangham, M. E., Lorenzini, E., and Vestal, L., "Tether Transportation System Study," NASA TP-1998-206959, March 1998.

[5]Forward, R., and Nordley, G., "Mars-Earth Rapid Interplanetary Tether Transport (MERITT) System: Initial Feasibility Analysis," *Journal of Propulsion and Power*, Vol. 17, No. 3, 2001, pp. 499–507.

[6]Johnson, L., and Herrmann, M., "International Space Station Electrodynamic Tether Reboost Study," NASA TM-1998-208538, July 1998.

[7]Vas, I. E., Kelly, T. J., and Scarl, E., "Application of an Electrodynamic Tether System to Reboost the International Space Station," *Proceedings of the Tether Technology Interchange Meeting*, NASA SP-1998-206900, Jan. 1998, pp. 305–334.

[8]Stuart, D. G., "Guidance and Control for Cooperative Tether-Mediated Orbital Rendezvous," *Journal of Guidance, Control, and Dynamics*, Vol. 13, No. 6, 1990, pp. 1102–1108.

[9]Bekey, I., "Tethering a New Technique for Payload Deployment," *Aerospace America*, Vol. 35, No. 3, 1997, pp. 36–40.

[10]Zimmerman, F., Schottle, U. M., and Messerschmid, E., "Optimal Deployment and Return Trajectories for a Tether-Assisted Re-Entry Mission," *AIAA Atmospheric Flight Mechanics Conference and Exhibit*, AIAA, Reston, VA, 1999, pp. 433–443; also AIAA Paper 99-4168.

[11]Longuski, J. M., Puig-Suari, J., and Mechalas, J., "Aerobraking Tethers for the Exploration of the Solar System," *Acta Astronautica*, Vol. 35, No. 2/3, 1995, pp. 205–214.

[12]Uphoff, C., and Janssens, F., "The Space Anchor: A Tethered Drag Device to Enhance Orbit Capture," *Proceedings of the AAS/AIAA Space Flight Mechanics Meeting*, Vol. 105, edited by C. A. Kleuver, B. Neta, C. D. Hall, and J. M. Hanson, Univelt, San Diego, 2000, pp. 1403–1425.

[13]Hoyt, R. P., and Forward, R. L., "The Terminator Tether™: Autonomous Deorbit of LEO Spacecraft for Space Debris Mitigation," AIAA Paper 2000-0329, Jan. 2000.

[14]Ruiz, M., Lopez-Rebollal, O., Lorenzini, E. C., and Pelaez, J., "Modal Analysis of the Stability of Periodic Solutions in Electrodynamic Tethers," *Proceedings of the AAS/AIAA Astrodynamics Conference*, Vol. 108, edited by L. A. D'Amario, L. L. Sackett, D. J. Scheeres, and B. G. Williams, Univelt, San Diego, 2001, pp. 1553–1570.

[15]Misra, A. K., and Modi, V. J., "A Survey on the Dynamics and Control of Tethered Satellite Systems," *Advances in the Astronautical Sciences*, Vol. 62, Univelt, San Diego, 1987, pp. 667–719.

[16]Rupp, C. C., "A Tether Tension Control Law for Tethered Subsatellites Deployed Along the Local Vertical," NASA TM X-64963, Sept. 1975.

[17]Monshi, N., Misra, A., and Modi, V. J., "On the Reel Rate Control of Retrieval Dynamics of Tethered Satellite Systems," *Proceedings of the 1st AAS/AIAA Annual Spaceflight Mechanics Meeting*, AIAA, Washington, DC, 1991, pp. 1053–1075.

[18]Misra, A. K., Xu, D. M., and Modi, V. J., "On Control of Tethered Satellite Systems," *IFAC Automatic Control in Space*, Pergamon, New York, 1985, pp. 145–151.

[19]Palaez, J., "On the Dynamics of the Deployment of a Tether From an Orbiter—I. Basic Equations," *Acta Astronautica*, Vol. 36, No. 2, 1995, pp. 113–122.

[20]Palaez, J., "On the Dynamics of the Deployment of a Tether From an Orbiter—Part II. Exponential Deployment," *Acta Astronautica*, Vol. 36, No. 6, 1995, pp. 313–335.

[21]Pascal, M., Djebli, A., and Bakkali, L. E., "A New Deployment/Retrieval Scheme for a Tethered Satellite System, Intermediate Between the Conventional Scheme and the Crawler Scheme," *Acta Astronautica*, Vol. 65, No. 4, 2001, pp. 689–696.

[22]Banerjee, A. K., and Kane, T. R., "Tethered Satellite Retrieval with Thruster Augmented Control," *Journal of Guidance, Control, and Dynamics*, Vol. 7, No. 1, 1984, pp. 45–50.

[23]Xu, D. M., Misra, A. K., and Modi, V. J., "Thruster-Augmented Active Control of a Tethered Subsatellite System During its Retrieval," *Journal of Guidance, Control, and Dynamics*, Vol. 9, No. 6, 1986, pp. 663–672.

[24]Chu, S., and Wang, L., "Strategy for the Passive Maneuvering of Tether-Connected Systems," *Journal of Guidance, Control, and Dynamics*, Vol. 20, No. 2, 1997, pp. 284–290.

[25]Fujii, H., and Ishijima, S., "Mission Function Control for Deployment and Retrieval of a Subsatellite," *Journal of Guidance, Control, and Dynamics*, Vol. 12, No. 2, 1989, pp. 243–247.

[26]Fujii, H. A., Uchiyama, K., and Kokubun, K., "Mission Function Control of Tethered Subsatellite Deployment/Retrieval: In-Plane and Out-of-Plane Motion," *Journal of Guidance, Control, and Dynamics*, Vol. 14, No. 2, 1991, pp. 471–473.

[27]Kim, E., and Vadali, S. R., "Nonlinear Feedback Deployment and Retrieval of Tethered Satellite Systems," *Journal of Guidance, Control, and Dynamics*, Vol. 15, No. 1, 1992, pp. 28–34.

[28]Vadali, S. R., "Feedback Tether Deployment and Retrieval," *Journal of Guidance, Control, and Dynamics*, Vol. 14, No. 2, 1991, pp. 469–470.

[29]Vadali, S. R., and Kim, E. S., "Feedback Control of Tethered Satellites Using Lyapunov Stability Theory," *Journal of Guidance, Control, and Dynamics*, Vol. 14, No. 4, 1991, pp. 729–735.

[30]Keshmiri, M., Misra, A. K., and Modi, V. J., "Control of Multi-Tethered Satellite Systems Using Lyapunov's Stability Theory," *AAS/AIAA Spaceflight Mechanics Meeting*, Vol. 89, edited by R. J. Proulx, J. J. F. Liu, P. K. Seidelmann, and S. Alfano, Univelt, San Diego, 1995, pp. 1161–1182.

[31]Fujii, H. A., and Anazawa, S., "Deployment/Retrieval Control of Tethered Subsatellite Through an Optimal Path," *Journal of Guidance, Control, and Dynamics*, Vol. 17, No. 6, 1994, pp. 1292–1298.

[32]Koakutsu, H., Nakajima, A., Ota, S., and Nakasuka, S., "Control of a Micro Tether System for Inducing Rotational Motion on Elliptical Orbit," *Proceedings of the 21st International Symposium on Space Technology and Science*, 21st International Space Technology and Science Publications Committee, Tokyo, Japan, 1998, pp. 755–762.

[33]Modi, V. J., Gilardi, G., and Misra, A. K., "Attitude Control of Space Platform Based Tethered Satellite System," *Journal of Aerospace Engineering*, Vol. 11, No. 2, 1998, pp. 24–31.

[34]Pradhan, S., Modi, V. J., and Misra, A. K., "Control of Tethered Satellite Systems Using Thruster and Offset Strategies," *International Journal of Control*, Vol. 64, No. 2, 1996, pp. 175–193.

[35]Pradhan, S., Modi, V. J., and Misra, A. K., "Tether-Platform Coupled Control," *Acta Astronautica*, Vol. 36, No. 2, 1999, pp. 243–256.

[36]Bergamaschi, S., and Quadrelli, B., "Magnetically Induced Librations in Conducting Tethers," *Proceedings of the AAS/AIAA Astrodynamics Conference*, Vol. 65, edited by J. K. Seldner, A. K. Misra, R. E. Lindberg, and W. Williamson, Univelt, San Diego, 1987, pp. 441–453.

[37]Lanoix, E. L. M., Misra, A. K., Modi, V. J., and Tyc, G., "Effect of Electromagnetic Forces on the Orbital Dynamics of Tethered Satellites," *Proceedings of the AAS/AIAA Space Flight Mechanics Meeting*, Vol. 105, edited by C. A. Kleuver, B. Neta, C. D. Hall, and J. M. Hanson, Univelt, San Diego, 2000, pp. 1347–1365.

[38]Pelaez, J., Ruiz, M., Lopez-Rebollal, O., Lorenzini, E. C., and Cosmo, M. L., "A Two Bar Model for the Dynamics and Stability of Electrodynamic Tethers," American Astronautical Society, Paper 00-188, Jan. 2000.

[39]Pelaez, J., Lorenzini, E. C., Lopez-Rebollal, O., and Ruiz, M., "A New Kind of Dynamic Instability in Electrodynamic Tethers," American Astronautical Society, Paper 00-190, Jan. 2000.

[40]Lorenzini, E. C., Estes, R. D., Cosmo, M. L., and Pelaez, J., "Dynamical, Electrical and Thermal Coupling in a New Class of Electrodynamic Tethered Satellites," *Proceedings of the 9th AAS/AIAA Spaceflight Mechanics Meeting*, Vol. 102, edited by R. H. Bishop, R. D. Culp, D. L. Machison, and M. J. Evans, Univelt, San Diego, 1999, pp. 1333–1344.

[41]Pelaez, J., Lopez-Rebollal, O., Ruiz, M., Lorenzini, E. C., and Cosmo, M. L., "On the Radial Oscillation of an Electrodynamic Tether," *Proceedings of the 9th AAS/AIAA Spaceflight Mechanics Meeting*, Vol. 102, edited by R. H. Bishop, R. D. Culp, D. L. Machison, and M. J. Evans, Univelt, San Diego, 1999, pp. 1361–1380.

[42]Netzer, E., and Kane, T. R., "Electrodynamic Forces in Tethered Satellite Systems, Part I: System Control," *IEEE Transactions on Aerospace and Electronic Systems*, Vol. 30, No. 4, 1994, pp. 1031–1043.

[43]Tani, J., and Qiu, J., "Motion Control of a Tethered Subsatellite Using Electromagnetic Force," *Proceedings of the Seventh International Conference on Adaptive Structures*, Technomic Pub., Lancaster, PA, 1996, pp. 321–330.

[44]Misra, A. K., Xu, D. M., and Modi, V. J., "On Vibrations of Orbiting Tethers," *Acta Astronautica*, Vol. 13, No. 10, 1986, pp. 587–597.

[45]Kim, E., and Vadali, S. R., "Modeling Issues Related to Retrieval of Flexible Tethered Satellite Systems," *Journal of Guidance, Control, and Dynamics*, Vol. 18, No. 5, 1995, pp. 1169–1176.

[46]Trivailo, P., Fujii, H., and Blanksby, C., "Safety Implications of Unsheduled Situations in the Operation of Tethered Satellite Systems From the International Space Station," *Acta Astronautica*, Vol. 44, Nos. 7–12, 1999, pp. 701–707.

[47]Ohstuka, T., and Yoshida, T., "Deployment/Retrieval Control Simulation of a Tethered Satellite with Mass and Flexibility," *11th Workshop on Astrodynamics and Flight Mechanics*, Inst. of Space and Astronautical Science, Sagamihara, Japan, 2001, pp. 281–286.

[48]Sanmartin, J. R., Martinez-Sanchez, M., and Ahedo, E., "Bare Wire Anodes for Electrodynamic Tethers," *Journal of Propulsion and Power*, Vol. 9, No. 3, 1993, pp. 353–360.

[49]von Flotow, A. H., "Travelling Wave Control for Large Space Structures," *Journal of Guidance, Control, and Dynamics*, Vol. 9, No. 4, 1986, pp. 462–468.

[50]Fujii, H. A., Ohtsuka, T., and Murayama, T., "Wave-Absorbing Control for Flexible Structures with Noncollocated Sensors and Actuators," *Journal of Guidance, Control, and Dynamics*, Vol. 15, No. 2, 1992, pp. 431–439.

[51]Fujii, H. A., and Ohtsuka, T., "Experiment of a Noncollocated Controller for Wave Cancellation," *Journal of Guidance, Control, and Dynamics*, Vol. 15, No. 3, 1992, pp. 741–745.

[52]Matsuda, K., and Fujii, H., "H_∞ Optimized Wave-Absorbing Control: Analytical and Experimental Results," *Journal of Guidance, Control, and Dynamics*, Vol. 16, No. 6, 1993, pp. 1146–1153.

[53]Fujii, H. A., Watanabe, T., Taira, W., and Trivailo, P., "An Analysis of Vibration and Wave-Absorbing Control of Tether Systems," AIAA Paper 2001-4033, Aug. 2001.

[54]Hoyt, R. P., "Stabilization of Electrodynamic Space Tethers," Space Technology and Applications International Forum, STAIF-2002, Feb. 2002.